

A Bipartite Graph Approach for FDD V2V Underlay Massive MIMO Transmission

Li You, *Member, IEEE*, Meng Xiao, Kezhi Wang, *Senior Member, IEEE*, Wenjin Wang, *Member, IEEE*,
and Xiqi Gao, *Fellow, IEEE*

Abstract—Utilizing the inherent sparsity of massive multiple-input multiple-output (MIMO) channels in the beam domain, we propose a bipartite graph approach for frequency-division duplexing (FDD) vehicle-to-vehicle (V2V) underlay massive MIMO transmission. First, the physically motivated constraints are introduced to schedule the users with channel dimension no larger than the pilot dimension and beam directions with strong channel power as well as weak interference. We then develop an optimization problem which is formulated as a mixed-integer linear program (MILP) to maximize the rank of the effective channel matrix subject to the introduced constraints. We further provide a channel estimation and precoding scheme for the base station and each V2V transmitter based on the equivalent reduced-dimensional channels which is the solution of MILP. Numerical results show the superiority of the proposed bipartite graph approach in terms of pilot overhead and spectral efficiency over the conventional baseline.

Index Terms—Massive MIMO, FDD, V2V, bipartite graph.

I. INTRODUCTION

Advanced vehicular technologies play a fundamental role in designing the wireless vehicle-to-everything (V2X) communications and demonstrate enormous potential in accelerating full deployment of Intelligent Transportation Systems (ITS) [1], [2]. However, with the dramatically increasing demand for safe driving, etc., the challenge of achieving substantial performance gains in spectral efficiencies is yet to be addressed. In addition, vehicle-to-vehicle (V2V) communications may be supported via utilizing device-to-device (D2D) and cellular-based communications [3]–[5]. Besides, frequency-division duplexing (FDD) system is widely recognized as an effective system for delay-sensitive applications and symmetric traffic.

Manuscript received November 10, 2020; revised February 19, 2021; accepted April 22, 2021. Date of publication XXXX, 2021; date of current version XXXX, 2021. This work was supported in part by the National Key R&D Program of China under Grant 2018YFB1801103; in part by the National Natural Science Foundation of China under Grants 61801114, 61631018, and 61761136016; in part by the Jiangsu Province Basic Research Project under Grant BK20192002; and in part by the Fundamental Research Funds for the Central Universities. The review of this paper was coordinated by Prof. Linglong Dai. (*Corresponding author: Xiqi Gao.*)

Li You, Meng Xiao, Wenjin Wang, and Xiqi Gao are with the National Mobile Communications Research Laboratory, Southeast University, Nanjing 210096, China, and also with the Purple Mountain Laboratories, Nanjing 211100, China (e-mail: liyou@seu.edu.cn; mxiao@seu.edu.cn; wang-wj@seu.edu.cn; xqgao@seu.edu.cn).

Kezhi Wang is with the Department of Computer and Information Sciences, Northumbria University, Newcastle upon Tyne, NE1 8ST, U.K. (e-mail: kezhi.wang@northumbria.ac.uk).

Color versions of one or more of the figures in this paper are available online at <http://ieeexplore.ieee.org>.

Digital Object Identifier

Thus, FDD V2V underlay¹ massive multiple-input multiple-output (MIMO) has become a promising technology for future generation networks since it can significantly increase the spectral efficiency by using massive antenna arrays [7]–[9].

For efficient massive MIMO transmission, it is essential to obtain the channel state information (CSI). The common setup for a massive MIMO system is that each cellular user (CUE) is only equipped with a few number of antennas, while the base station (BS) is equipped with an enormous number of antennas. In time-division duplexing (TDD) systems, the downlink (DL) CSI can be obtained by exploiting the inherent channel reciprocity between the uplink (UL) and DL. Unfortunately, channel reciprocity no longer holds for a FDD system due to the difference between frequencies which the UL and DL transmission operate at. For the considered FDD V2V underlay massive MIMO transmission, it is challenging to obtain the CSI due to the high overhead caused by fast V2V channel fading and large antenna arrays at the BS and V2V transmitters (VTs). To mitigate this issue, we explore the potential of representing the original high-dimensional channel with a reduced-dimensional equivalent one, since most of the channel power is concentrated in a limited number of beam directions in practical outdoor massive MIMO scenarios. In [10], the authors proposed an active channel sparsification method utilizing the bipartite graph formulation to reduce the original channel dimension for a single-cell transmission, which inspires us to apply the powerful mathematical tool, i.e., the bipartite graph for the considered FDD V2V underlay massive MIMO cellular network. Different from the single-cell transmission scenario [10], we take into account the mutual interference across the CUEs and V2V receivers (VRs).

In this paper, we first formulate a bipartite graph for FDD V2V underlay massive MIMO transmission. We introduce the constraints to schedule the users with channel dimension no larger than the desired pilot dimension and beam directions with strong channel power as well as weak inter-user interference. Then, we develop an optimization problem to maximize the rank of the effective channel matrix subject to the introduced constraints. The optimization problem can be efficiently solved by casting it as a mixed integer linear program (MILP). We further provide a channel estimation and precoding scheme for the BS and VTs over the equivalent

¹Note that there are two types of spectrum sharing between the V2V and cellular links: the underlay and overlay schemes [6]. Different from the overlay scheme where the V2V and cellular links utilize disjoint spectrum resources, the underlay scheme can utilize the spectrum more efficiently as both links share the spectrum resources.

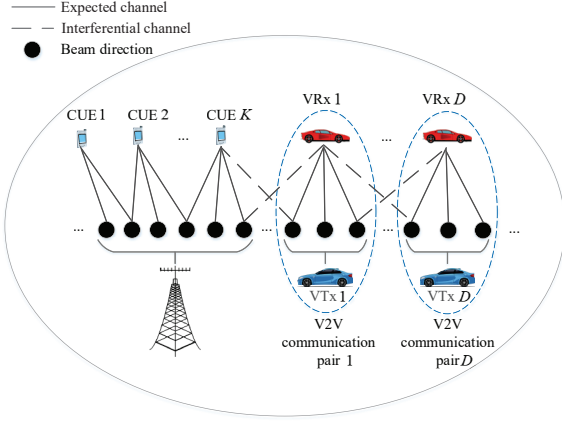


Fig. 1. A bipartite graph for V2V underlay massive MIMO system.

reduced-dimensional channels based on the solution of MILP. Simulation results demonstrate that the proposed bipartite graph approach can significantly improve the spectral efficiency over the conventional baseline.

II. SYSTEM MODEL

As shown in Fig. 1, we consider a single-cell FDD V2V underlay massive MIMO downlink system, which is composed of K single-antenna CUEs, a M -antenna BS, and D V2V communication pairs. The d -th V2V communication pair consists of a N_d -antenna VT and a single-antenna VR.² We assume that all users share the same time and frequency resources, and both the BS and VTs are equipped with massive antenna arrays, i.e., N_d and M are sufficiently large.

For frequency-flat and block-fading channels, we denote \mathbf{g}_k^{bc} , $\mathbf{g}_{l,k}^{\text{vc}}$, $\mathbf{g}_{l,d}^{\text{vv}}$, and \mathbf{g}_d^{bv} as the channel vectors from the BS to the k -th CUE, l -th VT to k -th CUE, l -th VT to d -th VR, and the BS to the d -th VR, respectively. According to [11], when the BS and VTs are equipped with massive antenna arrays, the channel covariance matrices can be well approximated by

$$\mathbf{R}_k^{\text{bc}} = \mathbb{E} \{ \mathbf{g}_k^{\text{bc}} (\mathbf{g}_k^{\text{bc}})^H \} \stackrel{M \rightarrow \infty}{\approx} \beta_k^{\text{bc}} \mathbf{V}_M \text{diag} \{ \mathbf{r}_k^{\text{bc}} \} \mathbf{V}_M^H, \quad (1a)$$

$$\mathbf{R}_{l,d}^{\text{vx}} = \mathbb{E} \{ \mathbf{g}_{l,d}^{\text{vx}} (\mathbf{g}_{l,d}^{\text{vx}})^H \} \stackrel{N_d \rightarrow \infty}{\approx} \beta_{l,d}^{\text{vx}} \mathbf{V}_{N_d} \text{diag} \{ \mathbf{r}_{l,d}^{\text{vx}} \} \mathbf{V}_{N_d}^H, \quad (1b)$$

where $x \in \{c, v\}$, β_k^{bc} and $\beta_{l,d}^{\text{vx}}$ denote the large-scale fading coefficients, \mathbf{V}_{N_d} and \mathbf{V}_M are both unitary matrices which depend on the topology of equipped massive antenna arrays. $\mathbf{r}_{l,d}^{\text{vx}}$ and \mathbf{r}_k^{bc} are vectors whose elements are related to the channel power angle spectrum (PAS).

Assume the channel covariance matrices of all CUEs and VRs are obtained by designing sounding pilot signals properly [11]. Besides, the channel elements follow the jointly Gaussian distribution according to the central limit theorem, i.e., $\mathbf{g}_k^{\text{bc}} \sim \mathcal{CN}(\mathbf{0}, \mathbf{R}_k^{\text{bc}})$ and $\mathbf{g}_{l,d}^{\text{vx}} \sim \mathcal{CN}(\mathbf{0}, \mathbf{R}_{l,d}^{\text{vx}})$.

²As the pilot overhead is not related to the number of receive antennas, we focus on the case with single-antenna VRs for brevity.

III. A BIPARTITE GRAPH APPROACH

To decrease the required number of pilot symbols and increase the spectral efficiency, we represent the high dimensional channel by an equivalent reduced-dimensional channel utilizing a bipartite graph model. Before proceeding, we first introduce some concepts which will be useful below [10]. In particular, ‘‘Maximal Matching’’ represents the largest subset of edges without common vertices. In addition, ‘‘Perfect Matching’’ represents a subset of edges which do not have common vertices and simultaneously cover all vertices.

A. Bipartite Graph Formulation

In this subsection, we investigate the formulation of a bipartite graph for V2V underlay massive MIMO transmission. For the bipartite graph in Fig. 1, the vertices on the top side represent CUEs and VRs, and those on the other side represent beams of the BS and VTs. Note that the edge between a user and a beam direction is connected when the beam is present in this user’s angular profile. In addition, edges between beams of the BS and CUEs (VTs and VRs in the same communication pair) represent the desired channels. Meanwhile, edges between beams of the BS and VRs (VTs and CUEs, or VTs and VRs in different communication pairs) denote the pilot or data interference.

Let $\mathbf{H}^{\text{bc}} = [\mathbf{r}_1^{\text{bc}}, \mathbf{r}_2^{\text{bc}}, \dots, \mathbf{r}_K^{\text{bc}}] \in \mathbb{C}^{M \times K}$, $\mathbf{H}^{\text{bv}} = [\mathbf{r}_1^{\text{bv}}, \mathbf{r}_2^{\text{bv}}, \dots, \mathbf{r}_D^{\text{bv}}] \in \mathbb{C}^{M \times D}$, $\mathbf{H}^{\text{vv}} = [\mathbf{r}_{i,j}^{\text{vv}}]_{D \times D} \in \mathbb{C}^{DN_d \times D}$ and $\mathbf{H}^{\text{vc}} = [(\mathbf{H}_1^{\text{vc}})^T, (\mathbf{H}_2^{\text{vc}})^T, \dots, (\mathbf{H}_D^{\text{vc}})^T]^T \in \mathbb{C}^{DN_d \times K}$, where $\mathbf{H}_i^{\text{vc}} = [\mathbf{r}_{i,1}^{\text{vc}}, \mathbf{r}_{i,2}^{\text{vc}}, \dots, \mathbf{r}_{i,K}^{\text{vc}}] \in \mathbb{C}^{N_d \times K}$ ($1 \leq i \leq D$) characterizes the statistical CSI. Denote $\mathbf{G} = \mathbf{H} \odot \mathbb{G} \in \mathbb{C}^{(M+DN_d) \times (K+D)}$ as the channel response matrix, where $\mathbf{H} = \begin{bmatrix} \mathbf{H}^{\text{bc}} & \mathbf{H}^{\text{bv}} \\ \mathbf{H}^{\text{vc}} & \mathbf{H}^{\text{vv}} \end{bmatrix}$, \odot denotes the Hadamard (elementwise) product, and \mathbb{G} is a random matrix with the elements being independently distributed as $\mathcal{CN}(0, 1)$. Let \mathbf{A}^{bc} , \mathbf{A}^{bv} , \mathbf{A}^{vv} , and \mathbf{A}^{vc} denote the one-bit thresholded version of \mathbf{H}^{bc} , \mathbf{H}^{bv} , \mathbf{H}^{vv} , and \mathbf{H}^{vc} , respectively. In other words, the element of matrix \mathbf{A} is 1 when the element at the corresponding position of matrix \mathbf{H} is greater than a suitable small threshold, and 0 otherwise. We consider a $(M+DN_d) \times (K+D)$ bipartite graph $\mathcal{L} = (\mathcal{A}, \mathcal{U}, \mathcal{E})$ with adjacency matrix $\mathbf{A} = \begin{bmatrix} \mathbf{A}^{\text{bc}} & \mathbf{A}^{\text{bv}} \\ \mathbf{A}^{\text{vc}} & \mathbf{A}^{\text{vv}} \end{bmatrix}$, in which \mathcal{A} , \mathcal{U} , and \mathcal{E} represent the sets of beam vertices, user vertices, and edges, respectively. Note that the weight of each edge in \mathcal{E} denotes the channel power and is decided by the eigenvalues of the corresponding channel.

Given a preset pilot dimension T_{dl} , we aim to form a sub-bipartite graph $\mathcal{L}' = (\mathcal{A}', \mathcal{U}', \mathcal{E}')$ of \mathcal{L} , which is required to satisfy the following constraints: 1) The vertex of each user or beam is connected to at least one desired edge, i.e., $N_{\mathcal{L}', \text{des}}(u) \geq 1, \forall u \in \mathcal{U}'$ and $N_{\mathcal{L}', \text{des}}(a) \geq 1, \forall a \in \mathcal{A}'$. 2) The number of edges in \mathcal{E}' incident to each user vertex in the selected subgraph is not larger than the pilot dimension, i.e., $N_{\mathcal{L}'}(u) \leq T_{\text{dl}}, \forall u \in \mathcal{U}'$. 3) The sum of weights of the desired edges in \mathcal{E}' incident to each user vertex in the selected subgraph accounts for a significant portion of the total channel power, i.e., $\sum_{a \in \mathcal{L}', \text{des}(u)} w_{a,u} \geq P_e, \forall u \in \mathcal{U}'$. 4) The sum of weights of the interfering edges in \mathcal{E}' incident to any user

vertex in the selected subgraph accounts for a small portion of the total channel power, i.e., $\sum_{a \in \mathcal{L}', \text{int}(u)} w_{a,u} \leq P_i, \forall u \in \mathcal{U}'$. 5) The channel response matrix $\mathbf{G}_{\mathcal{A}', \mathcal{U}'}$ composed of selected users and beam directions has a rank as large as possible. Note that the above constraints are different from those of the single-transmitter approach in [10].

We clarify the physical meaning of the above constraints as follows. In particular, the first constraint ensures that each user vertex is connected with at least one desired beam, and each beam vertex is connected with at least one desired user. The second constraint ensures that each of the selected effective channels can be efficiently estimated with the preset pilot length. The third constraint enables that the power of the expected channels of each selected CUE and VR accounts for most of the total channel power so that resources will not be wasted on serving users with weak expected channels. The fourth constraint ensures that the power of the interfering channel of each selected CUE and VR accounts for a small portion of the total channel power in order to control mutual interference among the users. Finally, the fifth constraint is designed to maximize the rank of the effective channel matrix $\mathbf{G}_{\mathcal{A}', \mathcal{U}'}$, which ultimately determines the beamforming gain and the number of spatially multiplexed data streams. Based on these results, the following lemma provides the convertibility between the rank of the effective matrix $\mathbf{G}_{\mathcal{A}', \mathcal{U}'}$ and a graph-theoretic quantity, namely, the size of the maximal matching.

Lemma 1 (Rank and Perfect Matchings [10]): For a given random matrix whose elements are either zero or drawn from a continuous distribution independently, its rank is given with probability 1 by the size of its largest intersection submatrix if and only if the bipartite graph of the largest intersection submatrix contains a perfect matching.

Note that the channel response matrix \mathbf{G} defined in subsection III-A has non-zero elements drawn from Gaussian distribution, which is in accordance with Lemma 1. However, different from the single-cell case in [10], the associated bipartite graph, as illustrated in Fig. 1, contains interfering edges which make no contribution to the beamforming and multiplexing gains. Therefore, we only consider a perfect matching composed of the expected edges. The bipartite graph formulation can be cast as the following optimization problem.

Problem 1: Denote by $\mathcal{M}(\mathcal{A}', \mathcal{U}')$ the matching composed of the expected edges in the sub-bipartite graph $\mathcal{L}' = (\mathcal{A}', \mathcal{U}', \mathcal{E}')$. Find the solution to the following problem:

$$\underset{\mathcal{A}' \subseteq \mathcal{A}, \mathcal{U}' \subseteq \mathcal{U}}{\text{maximize}} \quad |\mathcal{M}(\mathcal{A}', \mathcal{U}')| \quad (2a)$$

$$\text{subject to} \quad N_{\mathcal{L}', \text{des}}(a) \geq 1, \quad \forall a \in \mathcal{A}', \quad (2b)$$

$$N_{\mathcal{L}', \text{des}}(u) \geq 1, \quad \forall u \in \mathcal{U}', \quad (2c)$$

$$N_{\mathcal{L}'}(u) \leq T_{\text{dl}}, \quad \forall u \in \mathcal{U}', \quad (2d)$$

$$\sum_{a \in \mathcal{L}', \text{des}(u)} w_{a,u} \geq P_e, \quad \forall u \in \mathcal{U}', \quad (2e)$$

$$\sum_{a \in \mathcal{L}', \text{int}(u)} w_{a,u} \leq P_i, \quad \forall u \in \mathcal{U}'. \quad (2f)$$

In order to solve Problem 1 in a tractable way, we propose the following proposition.

Proposition 1: Problem 1 is equivalent to the following

MILP:

$$\underset{x_a, y_u, z_{a,u}}{\text{maximize}} \quad \sum_{a \in \mathcal{A}^c} \sum_{u \in \mathcal{U}^c} z_{a,u} + \sum_{d=1}^D \sum_{a \in \mathcal{A}_d^y} \sum_{u \in \mathcal{U}_d^y} z_{a,u} \quad (3a)$$

$$\text{subject to} \quad z_{a,u} \leq [\mathbf{A}]_{a,u}, \quad \forall u \in \mathcal{U}, \forall a \in \mathcal{A}, \quad (3b)$$

$$\sum_{u \in \mathcal{U}^c} z_{a,u} \leq x_a, \quad \forall a \in \mathcal{A}^c, \quad (3c)$$

$$\sum_{u \in \mathcal{U}_d^y} z_{a,u} \leq x_a, \quad \forall a \in \mathcal{A}_d^y, 1 \leq d \leq D, \quad (3d)$$

$$\sum_{a \in \mathcal{A}^c} z_{a,u} \leq y_u, \quad \forall u \in \mathcal{U}^c, \quad (3e)$$

$$\sum_{a \in \mathcal{A}_d^y} z_{a,u} \leq y_u, \quad \forall u \in \mathcal{U}_d^y, 1 \leq d \leq D, \quad (3f)$$

$$x_a \leq \sum_{u \in \mathcal{U}^c} [\mathbf{A}]_{a,u} y_u, \quad \forall a \in \mathcal{A}^c, \quad (3g)$$

$$x_a \leq \sum_{u \in \mathcal{U}_d^y} [\mathbf{A}]_{a,u} y_u, \quad \forall a \in \mathcal{A}_d^y, 1 \leq d \leq D, \quad (3h)$$

$$\begin{aligned} & \sum_{a \in \mathcal{A}^c} [\mathbf{A}]_{a,u} x_a + \sum_{d=1}^D \sum_{a \in \mathcal{A}_d^y} [\mathbf{A}]_{a,u} x_a \\ & \leq T_{\text{dl}} y_u + (M + DN_d)(1 - y_u), \quad \forall u \in \mathcal{U}^c, \end{aligned} \quad (3i)$$

$$\begin{aligned} & \sum_{d=1}^D \sum_{a \in \mathcal{A}_d^y} [\mathbf{A}]_{a,u} x_a + \sum_{a \in \mathcal{A}^c} [\mathbf{A}]_{a,u} x_a \\ & \leq T_{\text{dl}} y_u + (M + DN_d)(1 - y_u), \quad \forall u \in \mathcal{U}_d^y, 1 \leq d \leq D, \end{aligned} \quad (3j)$$

$$P_e y_u \leq \sum_{a \in \mathcal{A}^c} [\mathbf{W}]_{a,u} x_a, \quad \forall u \in \mathcal{U}^c, \quad (3k)$$

$$P_e y_u \leq \sum_{a \in \mathcal{A}_d^y} [\mathbf{W}]_{a,u} x_a, \quad \forall u \in \mathcal{U}_d^y, 1 \leq d \leq D, \quad (3l)$$

$$\sum_{d=1}^D \sum_{a \in \mathcal{A}_d^y} [\mathbf{W}]_{a,u} x_a \leq P_i y_u + \lambda N_d D (1 - y_u), \quad \forall u \in \mathcal{U}^c, \quad (3m)$$

$$\begin{aligned} & \sum_{a \in \mathcal{A}^c} [\mathbf{W}]_{a,u} x_a + \sum_{\substack{l=1 \\ l \neq d}}^D \sum_{a \in \mathcal{A}_l^y} [\mathbf{W}]_{a,u} x_a \leq P_i y_u + \lambda \\ & \cdot (M + DN_d - N_d)(1 - y_u), \quad \forall u \in \mathcal{U}_d^y, 1 \leq d \leq D, \end{aligned} \quad (3n)$$

$$x_a, y_u \in \{0, 1\}, \quad \forall a \in \mathcal{A}, u \in \mathcal{U}, \quad (3o)$$

$$z_{a,u} \in \{0, 1\}, \quad \forall a \in \mathcal{A}, u \in \mathcal{U}. \quad (3p)$$

Proof: See Appendix A. ■

The translated problem in (3) can be solved utilizing an off-the-shelf optimization toolbox efficiently. However, the optimal solution to Problem 1 is not necessarily unique. Thus, regularization can be adopted to determine the unique solution which has the same matching size as the optimal solution [10].

B. Channel Estimation and Precoding

In this subsection, we provide the channel estimation and precoding for the BS and VTs based on the solution of MILP given by $\{x_a\}_{a=1}^{M+DN_d}$ and $\{y_u\}_{u=1}^{K+D}$. We denote the set of selected beam directions' indices for the BS as $\mathcal{B}^c =$

TABLE I
SIMULATION SETUP PARAMETERS

Parameter	Value
Number of CUEs	8
Number of V2V communication pairs	1
Number of transmit antennas M, N_d	64
AS σ	2°

$\{a : x_a = 1, a \in \mathcal{U}^c\}$ with $|\mathcal{B}^c| = P^c$. Similarly, the set of selected beam directions' indices for the d th VTx is denoted by $\mathcal{B}_d^v = \{a : x_a = 1, a \in \mathcal{U}_d^v\}$ with $|\mathcal{B}_d^v| = P_d^v$. Then, the precoding matrices can be obtained as $\mathbf{B}^c = \mathbf{I}_{\mathcal{B}^c}^T \in \mathbb{C}^{P^c \times M}$ and $\mathbf{B}_d^v = \mathbf{I}_{\mathcal{B}_d^v}^T \in \mathbb{C}^{P_d^v \times N_d}$ where $\mathbf{I}_{\mathcal{B}}$ represents the submatrix of \mathbf{I} obtained by keeping the columns whose indices belong to \mathcal{B} . Hence, the equivalent reduced-dimensional channels between the k -th CUE and the d -th VR can be expressed as

$$\mathbf{B}^c \mathbf{g}_k^{\text{bc}} = \mathbf{g}_k^{\text{bc,eff}} \in \mathbb{C}^{P^c \times 1}, \quad \mathbf{B}_l^v \mathbf{g}_{l,k}^{\text{vc}} = \mathbf{g}_{l,k}^{\text{vc,eff}} \in \mathbb{C}^{P_l^v \times 1}, \quad (4a)$$

$$\mathbf{B}_l^v \mathbf{g}_{l,d}^{\text{vv}} = \mathbf{g}_{l,d}^{\text{vv,eff}} \in \mathbb{C}^{P_l^v \times 1}, \quad \mathbf{B}^c \mathbf{g}_d^{\text{bv}} = \mathbf{g}_d^{\text{bv,eff}} \in \mathbb{C}^{P^c \times 1}. \quad (4b)$$

Then, the non-zero elements of the equivalent reduced-dimensional channels of the k -th CUE or the d -th VR only exist at the entries belonging to \mathcal{B}^c and \mathcal{B}_d^v , which are known at the BS and the d -th VT. Constrained by (3i) and (3j), the dimensions of the total effective channel consisting of expected channels and interfering channels are not larger than the pilot dimension, T_{dl} , for each CUE and VR. Therefore, estimation of the effective channel vectors can be straightforwardly performed [10].

IV. SIMULATION RESULTS

In this section, we evaluate the channel estimation and spectral efficiency performance of the proposed bipartite graph approach for the FDD V2V underlay massive MIMO cellular system. We consider a typical outdoor wireless propagation environments with a truncated Laplacian channel PAS [11]. We assume that the channel angle spreads (ASs) σ are the same for all cellular and V2V users, and the mean channel angles of arrival (AoAs) of all transmitters distribute uniformly in a 120° sector. We adopt the large-scale fading model with the large-scale fading coefficient given by $\beta = d^{-\alpha_x}$ where “ d ” denotes the distance between the transmitter and the receiver, “ x ” denotes “ b ” or “ v ”, $\alpha_b = 3.76$ and $\alpha_v = 4.37$ are the pathloss exponents of the channels from the BS and VTs to receivers, respectively [4]. In the simulations, the distances from the BS and VTs to receivers are set as 100 m and 50 m, respectively. Then, the large-scale fading coefficients of the channels from BS and VTs to receivers are given by 3.01×10^{-8} and 3.76×10^{-8} , respectively. The transmit power of the BS and VTs during the pilot training and data transmission phases are set to be equal. The default simulation parameters are listed in Table I [4].

Fig. 2 plots the channel estimation performance for the conventional orthogonal pilot and the proposed bipartite graph

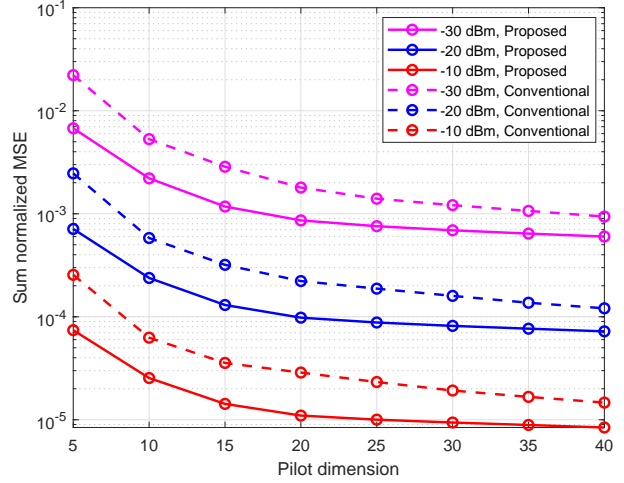


Fig. 2. Channel estimation performance comparison between the proposed bipartite graph and the conventional orthogonal pilot approaches for different transmit power.

approaches, respectively, for different transmit power.³ In particular, the sum normalized mean square error (MSE) performance of the cellular and V2V links is presented versus the pilot dimension. We can observe that the proposed approach provides channel estimation performance gain in terms of normalized MSE over the conventional one for a wide range of pilot dimensions.

In Fig. 3, we compare the sum achievable spectral efficiency performance between the two approaches against the pilot dimension for different transmit power. The channel coherence interval length is set as 80. By utilizing the proposed bipartite graph approach, we can achieve considerable system spectral efficiency with a small pilot overhead for massive MIMO. In contrast, for the conventional orthogonal pilot approach [10], the limited pilot dimension used for training can only serve for a small number of transmit antennas. As a result, the proposed approach provides significant spectral efficiency gains over the conventional orthogonal pilot one. In addition, we can observe that the sum spectral efficiency first increases then decreases with the pilot dimension as the pilot overhead gradually dominates the sum rate improvement.

Fig. 4 plots the sum achievable spectral efficiency performance between the two approaches versus the channel coherence interval length for different transmit power. For the conventional orthogonal approach, the pilot overhead is set to be 20%. It can be observed from Fig. 4 that the proposed bipartite graph approach provides significant spectral efficiency gains over the conventional orthogonal pilot one, especially in the high mobility case with small coherence interval lengths where the pilot overhead dominates.

V. CONCLUSION

In this paper, we proposed a bipartite graph approach for FDD V2V underlay massive MIMO transmission for reducing

³In the conventional orthogonal pilot approach, mutually orthogonal pilots are transmitted from all antennas of the BS and all VTs during the channel training phase [12].

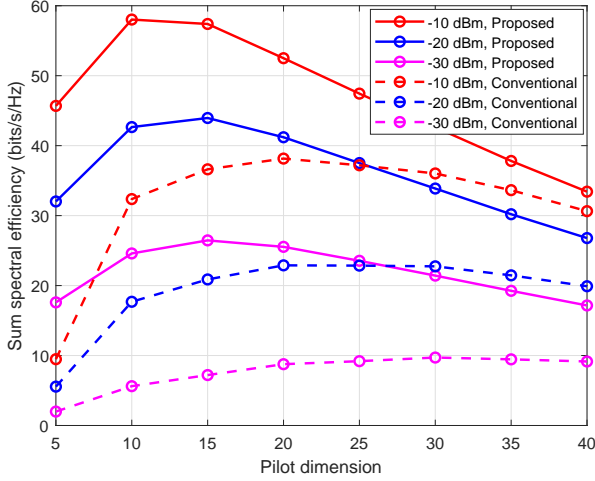


Fig. 3. Spectral efficiency performance comparison between the proposed bipartite graph and the conventional orthogonal pilot approaches for different transmit power.

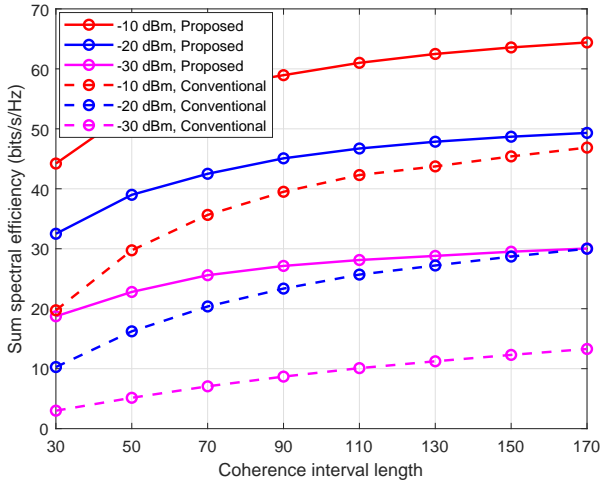


Fig. 4. Spectral efficiency performance comparison between the proposed bipartite graph and the conventional orthogonal pilot approaches for different transmit power.

the pilot overhead and increasing the spectral efficiency. We first investigated the bipartite graph formulation and introduced several constraints to select the effective users with channel dimension no large than the pilot length and beam directions with large channel power and weak interfering channel power. Then, we developed an optimization problem formulated as a MILP to maximize the rank of the effective channel matrix subject to the introduced constraints. In addition, based on the solution of MILP, we provided a channel estimation and precoding scheme over the equivalent reduced-dimensional channels for the BS and each VT. Simulation results demonstrated the spectral efficiency gain of the proposed bipartite graph approach over the conventional baseline.

APPENDIX A PROOF OF PROPOSITION 1

For convenience, we introduce the binary variables $\{x_a, a \in \mathcal{A}\}$ and $\{y_u, u \in \mathcal{U}\}$ to identify whether beam a and user u are selected, respectively. In addition, we divide the set of user vertices \mathcal{U} into $D + 1$ parts, which are expressed as \mathcal{U}^c and \mathcal{U}_d^v composed of all CUEs and the d th VR, respectively. Similarly, we denote the set of beam directions of the BS and the d th VT by \mathcal{A}^c and \mathcal{A}_d^v , respectively. Then, the constraints in (2b) and (2c) are equivalent to

$$x_a \leq \sum_{u \in \mathcal{U}^c} [\mathbf{A}]_{a,u} y_u, \quad \forall a \in \mathcal{A}^c, \quad (5a)$$

$$x_a \leq \sum_{u \in \mathcal{U}_d^v} [\mathbf{A}]_{a,u} y_u, \quad \forall a \in \mathcal{A}_d^v, 1 \leq d \leq D, \quad (5b)$$

$$y_u \leq \sum_{a \in \mathcal{A}^c} [\mathbf{A}]_{a,u} x_a, \quad \forall u \in \mathcal{U}^c, \quad (5c)$$

$$y_u \leq \sum_{a \in \mathcal{A}_d^v} [\mathbf{A}]_{a,u} x_a, \quad \forall u \in \mathcal{U}_d^v, 1 \leq d \leq D. \quad (5d)$$

Specifically, (5a) ensures that if beam a of the BS is selected, there must be some CUE $k \in \mathcal{U}^c$ such that the expected edges $(a, k) \in \mathcal{E}$ are selected. Similarly, in (5c), if the k -th CUE is selected, there must be some beam $a \in \mathcal{A}^c$ of the BS such that the expected edges $(a, k) \in \mathcal{E}$ are selected. (5b) ensures that if beam a of the d -th VT is selected, the d -th VR in the same pair must be selected. Similarly, in (5d), if the d -th VR is selected, there must be some beam $a \in \mathcal{A}_d^v$ of the d -th VT such that the expected edges $(a, d) \in \mathcal{E}$ are selected.

Moreover, the constraint in (2d) can be rewritten as:

$$\sum_{a \in \mathcal{A}^c} [\mathbf{A}]_{a,u} x_a + \sum_{d=1}^D \sum_{a \in \mathcal{A}_d^v} [\mathbf{A}]_{a,u} x_a \leq T_{d1} y_u + (M + DN_d)(1 - y_u), \quad \forall u \in \mathcal{U}^c, \quad (6a)$$

$$\sum_{d=1}^D \sum_{a \in \mathcal{A}_d^v} [\mathbf{A}]_{a,u} x_a + \sum_{a \in \mathcal{A}^c} [\mathbf{A}]_{a,u} x_a \leq T_{d1} y_u + (M + DN_d)(1 - y_u), \quad \forall u \in \mathcal{U}_d^v, 1 \leq d \leq D. \quad (6b)$$

In particular, (6a) and (6b) guarantee that if the k -th CUE or the d -th VR is scheduled, the number of edges incident to CUE k or VR d is no more than the pilot dimension. Meanwhile, the constraints in (2e) and (2f) can be rewritten as:

$$P_e y_u \leq \sum_{a \in \mathcal{A}^c} [\mathbf{W}]_{a,u} x_a, \quad \forall u \in \mathcal{U}^c, \quad (7a)$$

$$P_e y_u \leq \sum_{a \in \mathcal{A}_d^v} [\mathbf{W}]_{a,u} x_a, \quad \forall u \in \mathcal{U}_d^v, 1 \leq d \leq D, \quad (7b)$$

$$\sum_{d=1}^D \sum_{a \in \mathcal{A}_d^v} [\mathbf{W}]_{a,u} x_a \leq P_i y_u + \lambda N_d D (1 - y_u), \quad \forall u \in \mathcal{U}^c, \quad (7c)$$

$$\sum_{a \in \mathcal{A}^c} [\mathbf{W}]_{a,u} x_a + \sum_{\substack{l=1 \\ l \neq d}}^D \sum_{a \in \mathcal{A}_l^v} [\mathbf{W}]_{a,u} x_a \leq P_i y_u + \lambda$$

$$\cdot (M + DN_d - N_d)(1 - y_u), \forall u \in \mathcal{U}_d^v, 1 \leq d \leq D, \quad (7d)$$

where \mathbf{W} is the weighted adjacency matrix with the same dimension as \mathbf{A} , $[\mathbf{W}]_{a,u} = w_{a,u}$, and $\lambda = [\mathbf{W}]_{\max}$ represents the largest element in \mathbf{W} . (7a) and (7b) guarantee that if the k -th CUE or the d -th VR is selected, the sum weights of the selected expected beams of the BS and the d -th VT is no less than P_e . It is worth noting that the sum of weights of the interfering edges for the selected CUE k or VR d should be smaller than P_i , as indicated in (7c) and (7d).

To this end, another set of binary variables $\{z_{a,u}, a \in \mathcal{A}, u \in \mathcal{U}\}$ is introduced to indicate if an edge is selected to form the maximum matching composed of expected edges in $\mathcal{L}'(\mathcal{A}', \mathcal{U}', \mathcal{E}')$, i.e., $z_{a,u} = 1$. Following the canonical linear program formulation of the maximum cardinality matching for bipartite graphs, (2) can be translated into the following optimization problem:

$$\text{maximize}_{z_{a,u} \in \{0,1\}} \sum_{a \in \mathcal{A}^c} \sum_{u \in \mathcal{U}^c} [\mathbf{A}]_{a,u} z_{a,u} + \sum_{d=1}^D \sum_{a \in \mathcal{A}_d^v} \sum_{u \in \mathcal{U}_d^v} [\mathbf{A}]_{a,u} z_{a,u} \quad (8a)$$

$$\text{subject to} \sum_{u \in \mathcal{U}^c} [\mathbf{A}]_{a,u} z_{a,u} \leq 1, \forall a \in \mathcal{A}^c, \quad (8b)$$

$$\sum_{u \in \mathcal{U}_d^v} [\mathbf{A}]_{a,u} z_{a,u} \leq 1, \forall a \in \mathcal{A}_d^v, 1 \leq d \leq D, \quad (8c)$$

$$\sum_{a \in \mathcal{A}^c} [\mathbf{A}]_{a,u} z_{a,u} \leq 1, \forall u \in \mathcal{U}^c, \quad (8d)$$

$$\sum_{a \in \mathcal{A}_d^v} [\mathbf{A}]_{a,u} z_{a,u} \leq 1, \forall u \in \mathcal{U}_d^v, 1 \leq d \leq D, \quad (8e)$$

$$[\mathbf{A}]_{a,u} z_{a,u} \leq x_a, \forall u \in \mathcal{U}, \forall a \in \mathcal{A}, \quad (8f)$$

$$[\mathbf{A}]_{a,u} z_{a,u} \leq y_u, \forall u \in \mathcal{U}, \forall a \in \mathcal{A}, \quad (8g)$$

where (8f) and (8g) guarantee that the set of edges $\{(a, u) : z_{a,u} = 1\}$ of the matching is a subset of \mathcal{E}' , so that we can solve the problem on original setting \mathcal{L} rather than \mathcal{L}' . A further observation of the above constraints leads to the following equivalent simplified form:

$$\text{maximize}_{z_{a,u} \in \{0,1\}} \sum_{a \in \mathcal{A}^c} \sum_{u \in \mathcal{U}^c} z_{a,u} + \sum_{d=1}^D \sum_{a \in \mathcal{A}_d^v} \sum_{u \in \mathcal{U}_d^v} z_{a,u} \quad (9a)$$

$$\text{subject to} z_{a,u} \leq [\mathbf{A}]_{a,u}, \quad \forall u \in \mathcal{U}, \forall a \in \mathcal{A}, \quad (9b)$$

$$\sum_{u \in \mathcal{U}^c} z_{a,u} \leq x_a, \quad \forall a \in \mathcal{A}^c, \quad (9c)$$

$$\sum_{u \in \mathcal{U}_d^v} z_{a,u} \leq x_a, \quad \forall a \in \mathcal{A}_d^v, 1 \leq d \leq D, \quad (9d)$$

$$\sum_{a \in \mathcal{A}^c} z_{a,u} \leq y_u, \quad \forall u \in \mathcal{U}^c, \quad (9e)$$

$$\sum_{a \in \mathcal{A}_d^v} z_{a,u} \leq y_u, \quad \forall u \in \mathcal{U}_d^v, 1 \leq d \leq D, \quad (9f)$$

where the constraint added in (9b) makes $[\mathbf{A}]_{a,u} z_{a,u}$ in (8) and $z_{a,u}$ in (9) equivalent. The combination of constraints (8b), (8c), and (8f) contributes to the constraints (9c) and (9d). Similarly, the combination of constraints (8d), (8e), and (8g) contributes to the constraints (9e) and (9f). Thus, the eventual

MILP is concluded in (3).

ACKNOWLEDGMENT

The authors would like to thank the Associate Editor and the reviewers for their constructive comments and suggestions.

REFERENCES

- [1] L. Liang, H. Peng, G. Y. Li, and X. Shen, "Vehicular communications: A physical layer perspective," *IEEE Trans. Veh. Technol.*, vol. 66, no. 12, pp. 10 647–10 659, Dec. 2017.
- [2] Z. Gong, F. Jiang, and C. Li, "Angle domain channel tracking with large antenna array for high mobility V2I millimeter wave communications," *IEEE J. Sel. Topics Signal Process.*, vol. 13, no. 5, pp. 1077–1089, Mar. 2019.
- [3] H. Xu, W. Xu, Z. Yang, J. Shi, and M. Chen, "Pilot reuse among D2D users in D2D underlaid massive MIMO systems," *IEEE Trans. Veh. Technol.*, vol. 67, no. 1, pp. 467–482, Jan. 2018.
- [4] X. Liu, Y. Li, L. Xiao, and J. Wang, "Performance analysis and power control for multi-antenna V2V underlay massive MIMO," *IEEE Trans. Wireless Commun.*, vol. 17, no. 7, pp. 4374–4387, Jul. 2018.
- [5] L. You, M. Xiao, X. Song, Y. Liu, W. Wang, X. Q. Gao, and G. Fettweis, "Pilot reuse for vehicle-to-vehicle underlay massive MIMO transmission," *IEEE Trans. Veh. Technol.*, vol. 69, no. 5, pp. 5693–5697, May 2020.
- [6] F. Abbas, P. Fan, and Z. Khan, "A novel low-latency V2V resource allocation scheme based on cellular V2X communications," *IEEE Trans. Intell. Transp. Syst.*, vol. 20, no. 6, pp. 2185–2197, Jun. 2019.
- [7] Y. Chen, L. Wang, Y. Ai, B. Jiao, and L. Hanzo, "Performance analysis of NOMA-SM in vehicle-to-vehicle massive MIMO channels," *IEEE J. Sel. Areas Commun.*, vol. 35, no. 12, pp. 2653–2666, Dec. 2017.
- [8] H. Jiang, Z. Zhang, J. Dang, and L. Wu, "A novel 3-D massive MIMO channel model for vehicle-to-vehicle communication environments," *IEEE Trans. Commun.*, vol. 66, no. 1, pp. 79–90, Jan. 2018.
- [9] H. Jiang, Z. Zhang, L. Wu, J. Dang, and G. Gui, "A 3-D non-stationary wideband geometry-based channel model for MIMO vehicle-to-vehicle communications in tunnel environments," *IEEE Trans. Veh. Technol.*, vol. 68, no. 7, pp. 6257–6271, Jul. 2019.
- [10] M. Barzegar Khalilsarai, S. Haghghatshoar, X. Yi, and G. Caire, "FDD massive MIMO via UL/DL channel covariance extrapolation and active channel sparsification," *IEEE Trans. Wireless Commun.*, vol. 18, no. 1, pp. 121–135, Jan. 2019.
- [11] L. You, X. Q. Gao, X.-G. Xia, N. Ma, and Y. Peng, "Pilot reuse for massive MIMO transmission over spatially correlated Rayleigh fading channels," *IEEE Trans. Wireless Commun.*, vol. 14, no. 6, pp. 3352–3366, Jun. 2015.
- [12] T. L. Marzetta, "Noncooperative cellular wireless with unlimited numbers of base station antennas," *IEEE Trans. Wireless Commun.*, vol. 9, no. 11, pp. 3590–3600, Nov. 2010.